JACS
JOURNAL OF THE AMERICAN CHEMICAL SOCIETY
Article
pubs.acs.org/JACS

Specific Cell Surface Protein Imaging by Extended Self-Assembling Fluorescent Turn-on Nanoprobes

Keigo Mizusawa,[†] Yousuke Takaoka,[†] and Itaru Hamachi*[,†,‡]

[†]Department of Synthetic Chemistry and Biological Chemistry, Kyoto University, Katsura, Nishikyo-Ku, Kyoto 615-8510, Japan
[‡]Japan Science and Technology Agency (JST), CREST, 5 Sanbancho, Chiyoda-ku, Tokyo 102-0075, Japan

Supporting Information

ABSTRACT: Visualization of tumor-specific protein biomarkers on cell membranes has the potential to contribute greatly to basic biological research and therapeutic applications. We recently reported a unique supramolecular strategy for specific protein detection using self-assembling fluorescent nanoprobes consisting of a hydrophilic protein ligand and a hydrophobic BODIPY fluorophore in test tube settings. This method is based on recognition-driven disassembly of the nanoprobes, which induces a clear turn-on fluorescent signal. In the present study, we have successfully extended the range of applicable fluorophores to the more hydrophilic ones such as fluorescein or rhodamine by introducing a hydrophobic module near the fluorophore. Increasing the range of available fluorophores allowed selective imaging of membrane-bound proteins under live cell conditions. That is, overexpressed folate receptor (FR) or hypoxia-inducible membrane-bound carbonic anhydrases (CA) on live cell surfaces as cancer-specific biomarkers were fluorescently visualized using the designed supramolecular nanoprobes in the turn-on manner. Moreover, a cell-based inhibitor-assay platform for CA on a live cell surface was constructed, highlighting the potential applicability of the self-assembling turn-on probes.

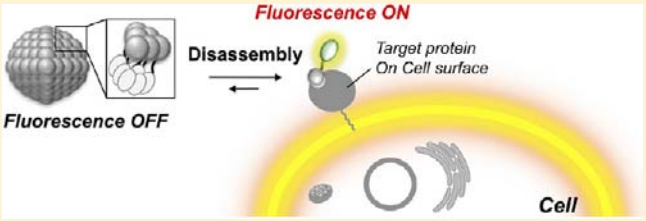

INTRODUCTION

Tumor-specific or tissue-selective protein biomarkers overexpressed on cell surfaces are important targets for basic biological research studies and therapeutic applications.[1] In most cases, antibodies appended with fluorescent molecules are used to visualize these endogenous biomarkers on live cells. However, they are always fluorescent, which inevitably requires a lot of washing operations for accurate molecular imaging on cells. Introduction of a switching mechanism (of fluorescent intensity and/or wavelength change only responsive to the target protein) should greatly help to solve this problem.[2] Recently, Urano and co-workers achieved highly specific *in vivo* cancer visualization using an antibody conjugated with novel acidic pH-activatable fluorescent probes.[3] Although undoubtedly valuable, such antibody-based probes possess several inherent problems, that is, besides their high cost, only a few antibodies can be prepared in large amounts, and site-specific, quantitative conjugation without loss of the antibody specificity remains difficult. On the other hand, small-molecule-based switchable fluorescent probes for the specific target proteins are particularly promising for imaging biomarkers, because they allow rapid, sensitive, and selective detection. The most prevalent probes are fluorogenic substrates that monitor the corresponding enzyme activity. However, this strategy can only be applied to particular enzymes (e.g., proteases or glycosidases),[4,5] not nonenzymatic proteins including the myriad of receptors in living systems. Clearly, establishment of a more general switching strategy for protein-specific fluorescent probes is highly desired.

Recently, several supramolecular approaches using amphiphilic polymers or dendrons for protein detection have been reported.[6,7] Although these nanomaterials are useful for protein sensing and profiling in a test tube context, they cannot be used for protein sensing under the crude cellular conditions because of their low selectivity or sensitivity to date. We also recently developed a disassembly-driven turn-on nanoprobe for specific protein detection.[8,9] The ligand-tethered fluorophores exhibited unique self-assembling features and showed the clear turn-on fluorescence change with high protein sensitivity.[9] However, only the hydrophobic fluorophore BODIPY was valid in our fluorescent probes, which greatly hampered their live cell application. Herein we extend the range of usable fluorophores to the more hydrophilic ones such as fluorescein or rhodamine by introducing a hydrophobic module near the fluorophore in the turn-on nanoprobe. Using the newly synthesized self-assembling fluorescent nanoprobes, we succeeded in imaging cancer-specific biomarkers such as the folate receptor (FR) and transmembrane-type carbonic anhydrases (CA) under a live cell setting (Scheme 1). Furthermore, a cell-based inhibitor screening system for CAs under hypoxic live cell conditions was successfully constructed.

Received: May 2, 2012
Published: July 18, 2012

dx.doi.org/10.1021/ja304239g | J. Am. Chem. Soc. 2012, 134, 13386−13395

Scheme 1. Schematic Illustration of a Self-Assembling Turn-on Fluorescent Probe for Cell Surface Protein Imaging

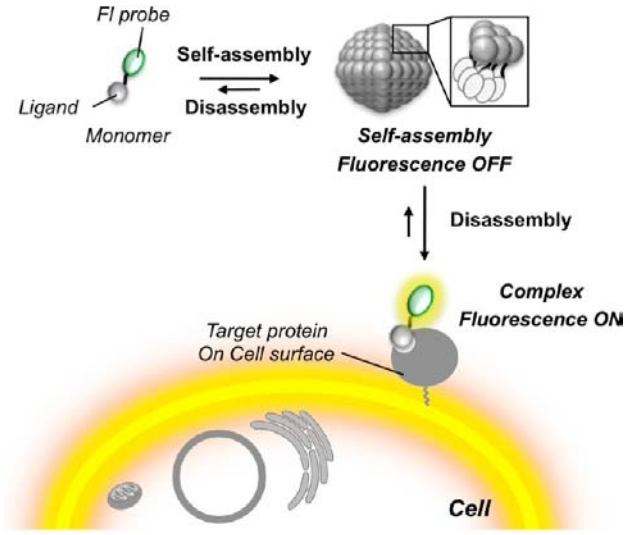

RESULTS AND DISCUSSION

Self-Assembling BODIPY-Based Fluorescent Probes toward DHFR Detection and FR Imaging. FR, a membrane-bound protein that is a potential biomarker because of its overexpression among malignant tumor cells, was the first target in a proof-of-principle experiment.[10] Using our previous design strategy, we newly prepared a turn-on fluorescent probe **1** to image FR. This probe consists of three modules: (i) a hydrophilic ligand specific to a protein of interest (methotrexate (MTX) as the ligand with an affinity for FR[11]), (ii) a fluorescent BODIPY as both a detection modality and a hydrophobic core, and (iii) a relatively hydrophobic linker group to connect these two modules and control the hydrophilic/hydrophobic balance (Figure 1a).

To test the turn-on property of probe **1** *in vitro*, we initially employed purified dihydrofolate reductase (DHFR) as a water-soluble model protein which can bind the MTX ligand in the same way as FR.[12] As shown in Figure 1b, the emission was extremely weak when **1** was dissolved in aqueous solution, but dramatically increased (by 23 times) upon the addition of DHFR. That is, probe **1** was an ideal off/on type of fluorescent

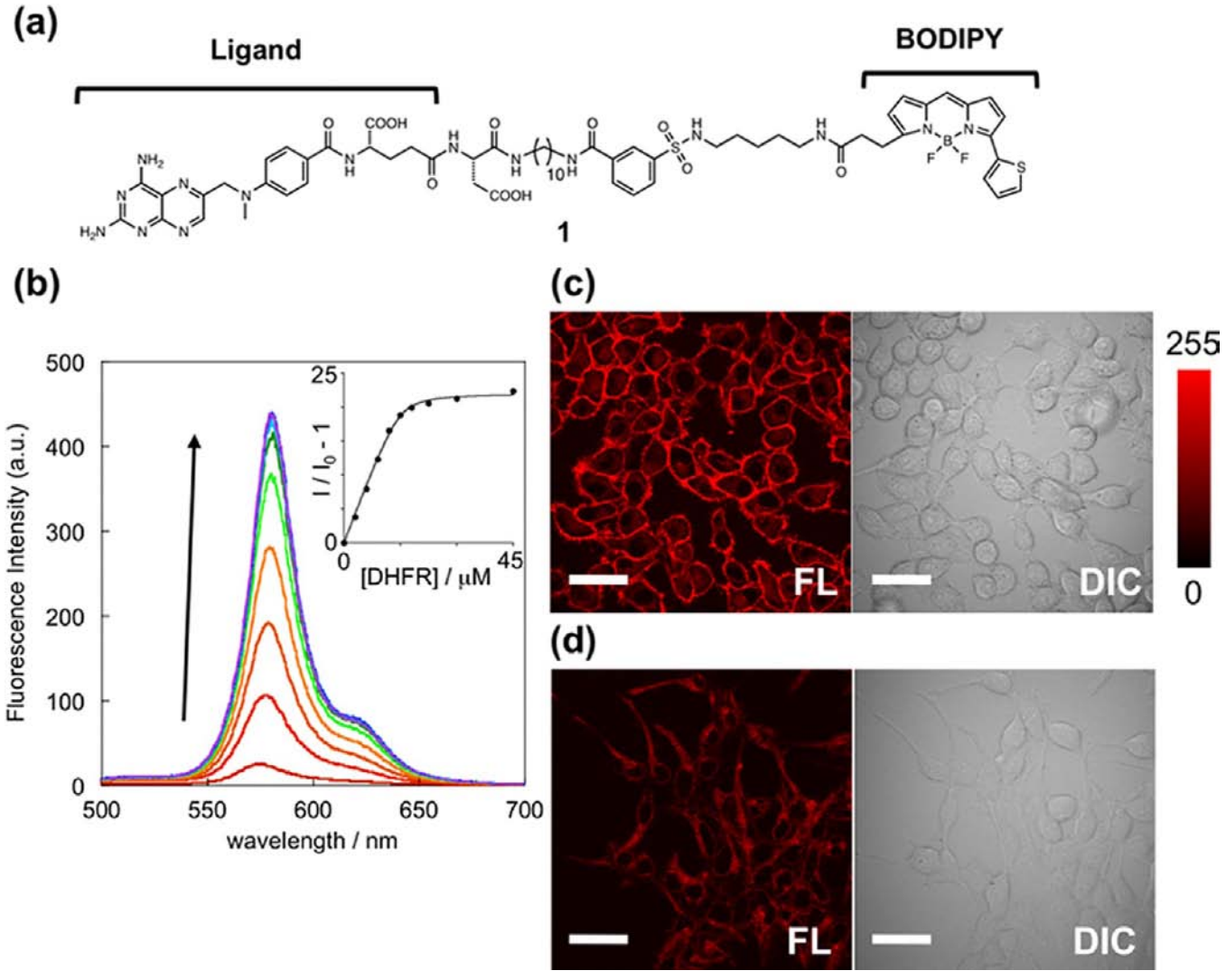

Figure 1. MTX-type BODIPY probe **1** for DHFR detection in the test tube and for FR imaging on live cell surfaces. (a) Chemical structure of probe **1**. (b) Fluorescence spectral changes of probe **1** (15 μM) upon addition of DHFR (0–45 μM) in test tube (λ_{ex} = 480 nm). (c, d) Fluorescence (left, FL) and differential interference images (right, DIC) of (c) KB cells or (d) HEK293T cells treated with probe **1** (15 μM). Scale bars, 40 μm.

dx.doi.org/10.1021/ja304239g | J. Am. Chem. Soc. 2012, 134, 13386–13395

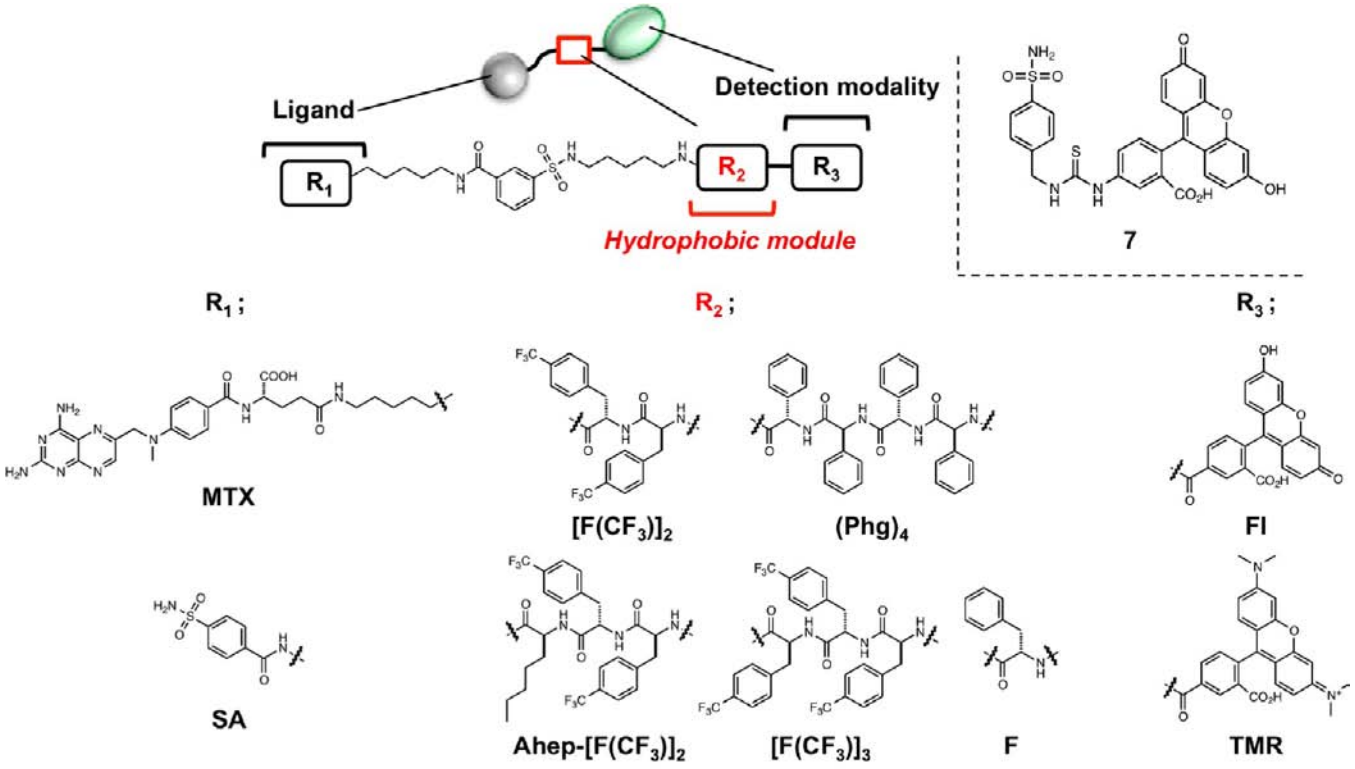

	2	3	4	5	6	8
R_1	MTX	MTX	MTX	MTX	SA	SA
R_2	-	$[F(CF_3)]_2$	$(Phg)_4$	F	Ahep-$[F(CF_3)]_2$	$[F(CF3)]_3$
R_3	Fl	Fl	Fl	TMR	Fl	Fl

Figure 2. Chemical structures of self-assembling probes based on hydrophilic fluorophores for FR and CA imaging: **2**–**5** for FR and **6**–**8** for hCAs.

probe for DHFR at least in test tube settings. We next applied **1** to live cell imaging of KB cells overexpressing FR.[13] Unfortunately, when a solution of **1** was added to the cultured KB cells, strong emission was observed inside the cells as well as on the cell surfaces in confocal laser scanning microscopy (CLSM) images (Figure 1c). The strong emission was also observed by using **1** even in the presence of an excess amount of folate, which is a competitive ligand for FR (Figure S1, Supporting Information [SI]). In addition, similar bright fluorescence was detected when **1** was mixed with HEK293T cells that did not express FR (Figure 1d).[14] It is clear that probe **1** could not selectively image FR, mainly due to its nonspecific binding to cell membranes and its cell permeability. These results indicate that both the turn-on fluorescent property and efficient suppression of nonspecific binding to cells should be considered for application of the self-assembled nanoprobes in live cell imaging.

Design of Fluorescein-Based Self-Assembling Turn-on Probes by Introduction of a Hydrophobic Module. To suppress nonspecific binding to live cell membranes, the fluorophore module was changed from the rather hydrophobic BODIPY to an anionic fluorescein (Fl). Similar to **1**, Fl-type probe **2** was composed of a simple sulfonamide linker for connecting MTX ligand and Fl (Figure 2). However, **2** alone showed a relatively large fluorescence (its fluorescence quantum yield (Φ) was 0.11), and thus the fluorescence enhancement induced by addition of DHFR was only 3.5-fold (Φ = 0.36) (Figure S2c, [SI]). That is, the inherent fluorescence of **2** was not efficiently quenched, probably because of the strong hydrophilicity of the Fl group, and thus this probe was identified as an always-on type of probe. To achieve more effective quenching, hydrophobic dipeptide (di-(4-trifluoromethyl-phenylalanine), $[F(CF_3)]_2$) was introduced as an additional hydrophobic module adjacent to the fluorophore in the Fl-type probe (probe **3**). As expected, the emission of **3** dissolved in aqueous solution was sufficiently weak (Φ = 0.03), and dramatically increased (by 10 times) upon addition of DHFR (Φ = 0.25, Figure 3b and c). Atomic force microscopy (AFM) images revealed the formation of spherical or oval aggregates of **3** with diameters ranging from 10 to 50 nm (Figure 3d). In dynamic light scattering (DLS) measurements, a buffer solution containing only **3** showed aggregates with a mean diameter of 30 nm (Figure 3e), whereas negligible scattering intensity was observed after addition of DHFR to this solution. These results indicate that probe **3** works as an ideal off/on type of probe driven by the recognition-triggered disassembly in the test tube. On the other hand, probe **4** containing a more hydrophobic tetrapeptide (tetra-phenylglycine, $(Phg)_4$, Figure 2) as the hydrophobic module exhibited almost no fluorescence both in the absence (Φ = 0.02) and presence of DHFR (Φ = 0.04, Figure 3c and Figure S2d [SI]), which classified **4** into an

dx.doi.org/10.1021/ja304239g | J. Am. Chem. Soc. 2012, 134, 13386–13395

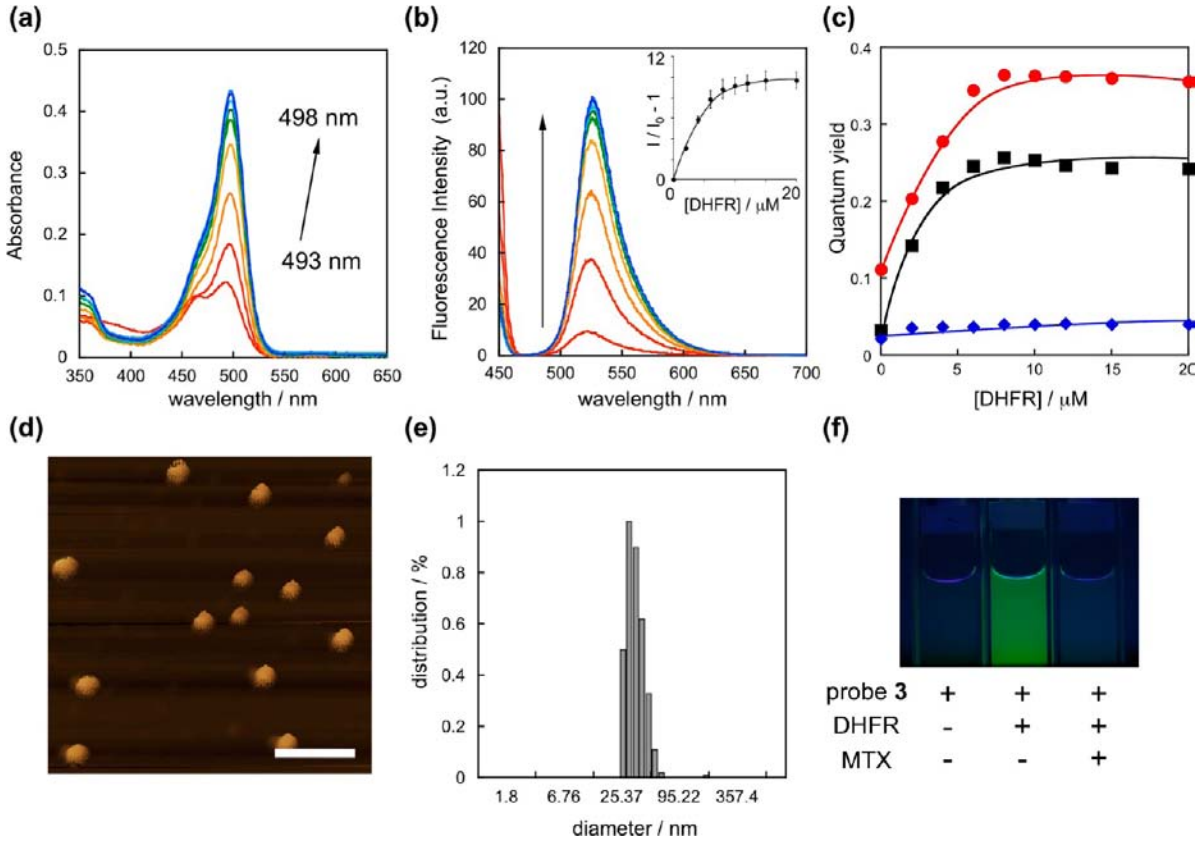

Figure 3. (a) UV−vis absorption spectral changes of probe **3** (10 μM) upon addition of DHFR (0−20 μM). (b) Fluorescence spectral changes of probe **3** (10 μM) upon addition of DHFR (0−20 μM) (λ_{ex} = 450 nm). (c) The fluorescence titration curves of **2** (●, red), **3** (■, black), or **4** (◆, blue) following addition of DHFR in test tube experiments. (d) AFM image of probe **3** only (10 μM, scale bar 200 nm). (e) DLS analysis of probe **3** only (10 μM). (f) Photographs of probe **3** (10 μM) in the absence (left) and presence (middle) of DHFR (10 μM), and after addition of MTX (100 μM) to the solution of **3** and DHFR (right). These images were obtained under UV excitation (λ_{ex} = 365 nm). All experiments were performed in 50 mM HEPES buffer (pH 7.2, 150 mM NaCl).

always-off type of probe (Table 1 and Figure S3 [SI]). Given all results in the Fl-type probes, it is clear that control of the hydrophobicity in the tail group containing hydrophilic fluorescein is critical for designing an ideal off/on type of fluorescent probe. In our previous study on ^{19}F NMR/MRI probes, we reported that the stability of aggregates was controlled by the hydrophobicity/hydrophilicity balance, which was crucial for an off/on ^{19}F NMR response.[8b] The present findings imply that a similar strategy is valid for fluorescence signal switching in the self-assembling probes. In the case of tetramethyl rhodamine (TMR) as another hydrophilic fluorophore, we indeed successfully developed the off/on type of probe **5** by introduction of phenylalanine as a hydrophobic module (Figures 2 and 4). Probe **5** (10 μM) exhibited a 37-fold enhancement of fluorescence from TMR at 584 nm upon addition of one equivalent of DHFR. This demonstrated that incorporation of a hydrophobic unit adjacent to the hydrophilic fluorophore is a general strategy to produce turn-on self-assembling fluorescent nanoprobes.

Table 1. Hydrophobic Modules and Response Patterns of Fluorescein-Type Probes[a]

probe	target[b]	hydrophobic module[b]	Φ without protein	Φ with protein	response patterns
2	FR/ DHFR	–	0.111	0.356	always-on
3	FR/ DHFR	$[F(CF_3)]_2$	0.032	0.251	off/on
4	FR/ DHFR	$(Phg)_4$	0.021	0.040	always-off
6	hCAs	Ahep-$[F(CF_3)]_2$	0.042	0.342	off/on
7	hCAs	–	0.457	0.423	always-on
8	hCAs	$[F(CF_3)]_3$	0.057	0.078	always-off

[a]Quantum yields were calculated by using fluorescein as a reference standard in test tube settings. [b]FR: folate receptor; DHFR: dihydrofolate reductase; hCAs: human carbonic anhydrases; $F(CF_3)$: 4-trifluoromethyl-phenylalanine; Phg: phenylglycine; Ahep: 2-amino-heptanoic acid.

MTX−Fluorescein-Type of Turn-on Probe for Fluorescent FR Imaging on Live Cell Surfaces. With the Fl-type of turn-on probe **3** in hand, we again set out to image FR on live cells. When probe **3** was added to KB cells, strong fluorescence in the CLSM image was observed only from the cell surface without requiring any washing operations (Figure 5a). The intensity of fluorescence on the cell surface decreased dramatically upon addition of folate without any change in the intensity of fluorescence in the extracellular region (Figure 5b). These data clearly indicate that turn-on fluorescence switching took place on live KB cell surface, and that this switching is reversible and controlled by the recognition of FR by the ligand moiety of **3**. In addition, probe **3** is not cell permeable, allowing FR to be visualized specifically on the cell surface. On the other hand, when DHFR was added to the solution containing KB

dx.doi.org/10.1021/ja304239g | J. Am. Chem. Soc. 2012, 134, 13386−13395

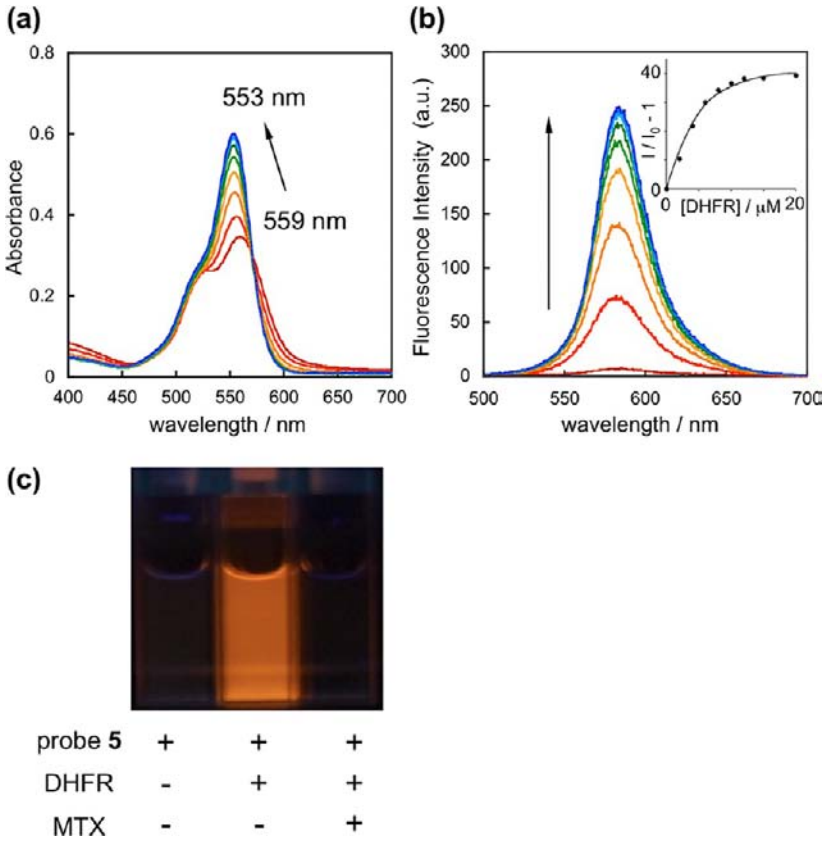

Figure 4. (a) UV−vis absorption spectra changes of TMR-type probe **5** (10 μM) upon addition of DHFR (0−20 μM). (b) Fluorescence spectra changes of probe **5** (10 μM) upon addition of DHFR (0−20 μM) (λ_{ex} = 480 nm). (c) Photographs of probe **5** (10 μM) in the absence (left) and presence (middle) of DHFR (10 μM), and after addition of MTX (100 μM) to the solution of **5** and DHFR (right). These images were obtained under UV excitation (λ_{ex} = 365 nm). All experiments were performed in 50 mM HEPES buffer (pH 7.2, 150 mM NaCl).

cells stained with **3**, the strong emission from the extracellular region was observed (Figure 5c). This data explicitly reveal that an excess amount of residual probe **3** forms self-assembled aggregates in solution, which retained the fluorescence signal-off state. Besides, no substantial fluorescence was observed from HEK293T cells with **3** (Figure 5d). All of the results demonstrate that the probe **3** is capable of specific fluorescent imaging of endogenous FR in a turn-on manner, unlike the original BODIPY-type probe **1**. Importantly, probe **3** efficiently suppressed the background signal from the extracellular region even under cellular conditions. By contrast, the higher background signals were observed from the extracellular region using the always-on-type probe **2**, whereas no detectable signals were observed with the use of the always-off type probe **4** (Figure S4, [SI]). These data supported that an ideal off/on type of probe could be synthesized by control of the self-assembling properties which would enable us to perform rapid live cell imaging of FR without requiring any extra operations.

Development of Sulfonamide−Fluorescein-Type Probe for Fluorescent Transmembrane-Type CA Imaging under Hypoxic Live Cell Conditions. Benefiting from the modular design, a self-assembling nanoprobe was constructed for fluorescent live cell imaging of another membrane protein. It has been reported that transmembrane-type human carbonic anhydrases (hCA IX and XII) are substantially overexpressed in response to the hypoxia inducible factor (HIF-1) in tumors.[15] Recent studies have also shown that CA IX is involved in tumorigenesis through pH regulation, and manipulation of cell proliferation and cell adhesion, making it a valuable target for cancer diagnostics and treatment.[16,17] On the basis of the same strategy as for the FR probes, off/on type probe **6** containing a benzenesulfonamide (SA) ligand for selective binding to the CA family was developed. In this case, hydrophobic tripeptide (2-aminoheptanoic acid and di-(4-trifluoromethyl-phenylalanine), Ahep-[F(CF_3)]$_2$, Figure 2), as the hydrophobic module was found to produce an ideal off/on type of probe (9-fold increase in fluorescent intensity, shown in a and b of Figure 6 and Figure S5 [SI]) in test tube experiments by evaluating the fluorescence response to hCA II, a soluble model of hCA IX. As in the case of the FR probes, always-on and always-off probes were also found among these CA probe candidates (Figure 2, Table 1, and Figure S6 [SI]) by varying the hydrophobic tail group.

Subsequently, imaging of the CA family on live cell surfaces was conducted using probe **6**. The A549 cell line was chosen, owing to its relatively high endogenous expression of hCA IX or XII under hypoxic conditions.[15a] Three parallel sets of A549 cells were respectively cultured for 24 h under hypoxic (<0.1% O_2), hypoxic-mimetic (in the presence of deferoxamine mesylate (DFO)), or normoxic conditions (20% O_2). When **6** was added to A549 cells cultured under the hypoxic conditions, strong emission was observed from the cell surface without any washing operations (Figure 6c).[18] The intensity of fluorescence decreased dramatically upon addition of ethoxazolamide (EZA), a strong inhibitor for CAs (Figure 6d). Similar clear fluorescent images were obtained from the cells incubated in the presence of DFO (Figure 6e), whereas significantly weaker emission was observed from A549 cell

dx.doi.org/10.1021/ja304239g | J. Am. Chem. Soc. 2012, 134, 13386−13395

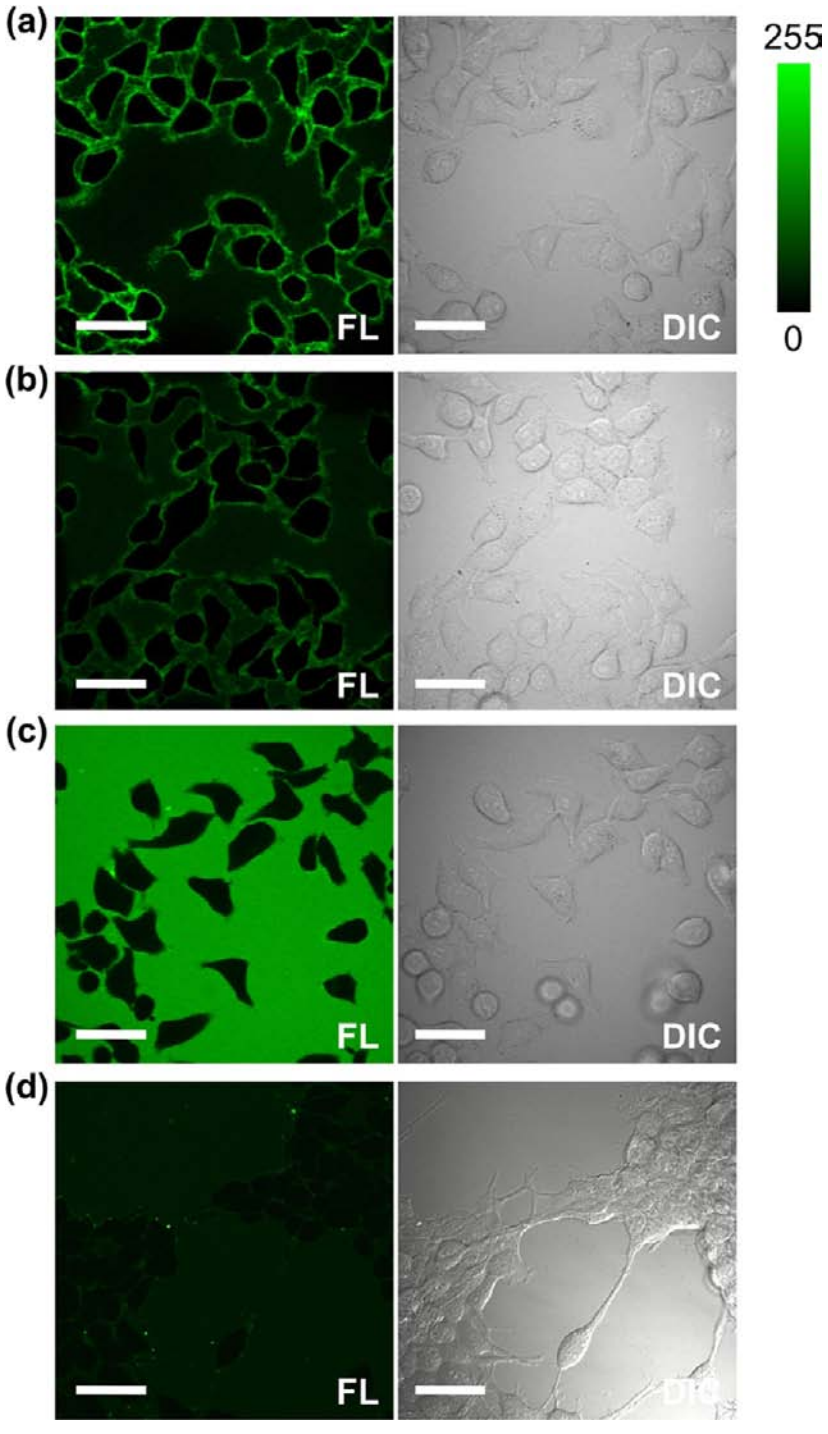

Figure 5. (a, b) Fluorescence images of KB cells treated with probe **3** (20 μM) in the (a) absence or (b) presence of folate (20 μM). (c) Fluorescence image of KB cells treated with probe **3** (20 μM) with purified DHFR (5 μM). (d) Fluorescence image of HEK293T cells treated with probe **3** (20 μM). Scale bars, 40 μm. Fluorescence imaging experiments were performed 1 min after the addition of the probe solution to the cells.

surfaces under normoxia (Figure 6f). In addition, negligible fluorescence was observed from HEK293T cells not expressing hCA IX (Figure S7, SI). Given all the data, we concluded that the probe **6** is capable of sensing not only the expression of the transmembrane-type hCA family but also the hypoxic environmental change of cancer cells based on the level of overexpression of the biomarkers.

Finally, imaging-based drug screening for hypoxia-inducible CAs was performed on live A549 cells using fluorescein-type probe **6**. After staining with **6** (10 μM), the A549 cells were mixed with several CA inhibitors, and changes in fluorescence images were monitored by CLSM without any washing operations. When the strong inhibitor EZA (100 nM) was added to the culture medium, a significant decrease in fluorescent intensity at the cell surface was induced with typical saturation behavior (Figure 7a). In the case of moderate inhibitors AAZ and SA-Py, the change in the CLSM image was saturated at 5 and 100 μM, respectively (b and c of Figure 7 and Figure S8, SI). In contrast, a very small change was observed upon addition of a higher concentration of 4-

dx.doi.org/10.1021/ja304239g | J. Am. Chem. Soc. 2012, 134, 13386−13395

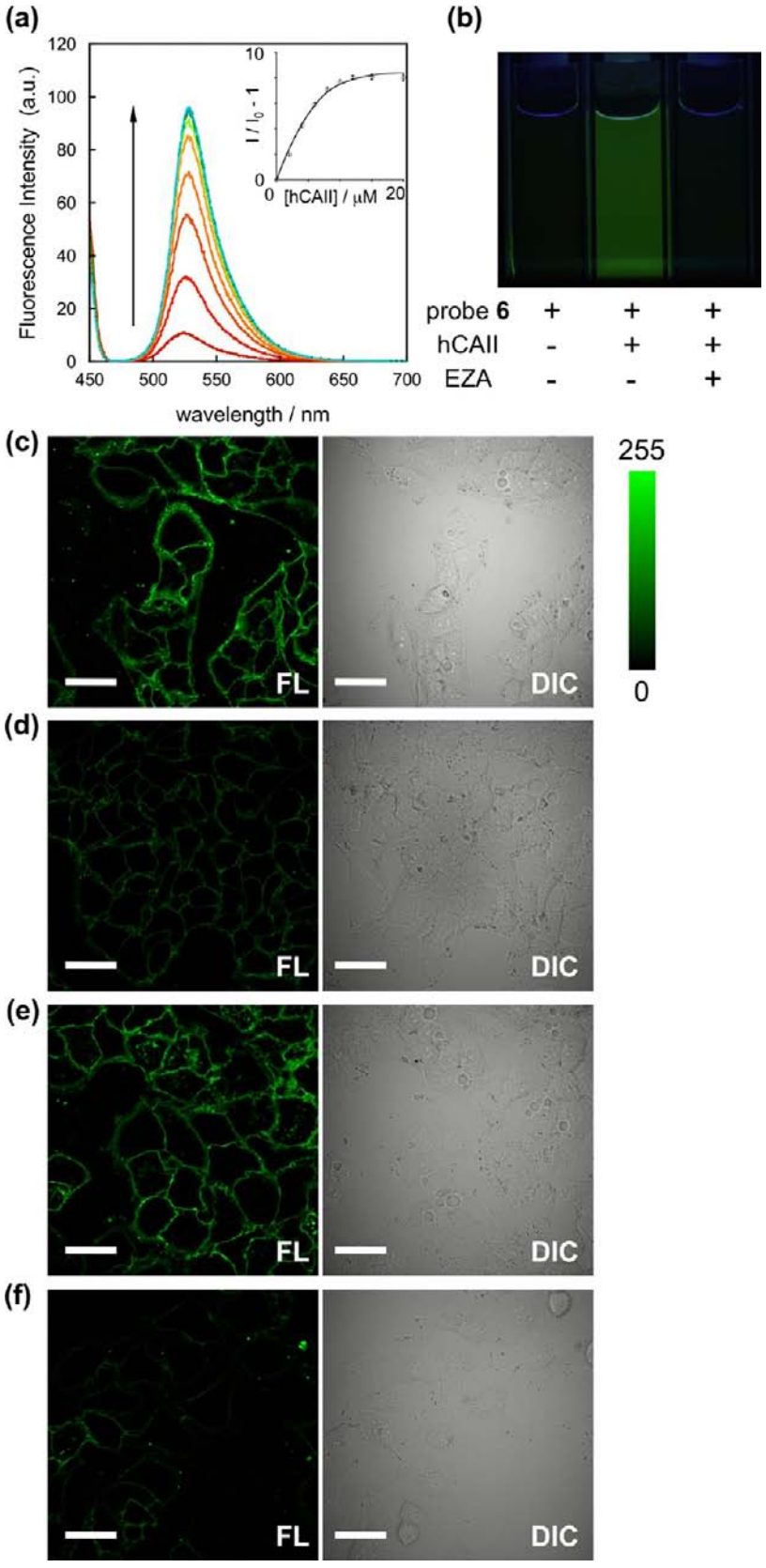

Figure 6. (a, b) Turn-on detection of hCAII with probe **6** in test tube settings. (a) Fluorescent spectral changes of probe **6** (10 μM) upon addition of hCAII (0−20 μM). (b) Photographs of probe **6** (10 μM) in the absence (left) and presence (middle) of hCAII (10 μM), and after addition of EZA (100 μM) to the solution of **6** and hCAII (right). (c, d) Transmembrane-type hCA imaging of A549 cells using probe **6** (10 μM) (c) without or (d) with EZA (100 μM) cultured under hypoxic conditions. (e) Transmembrane-type hCA imaging of DFO-treated A549 cells using probe **6** (10 μM). (f) Transmembrane-type hCA imaging of A549 cells using probe **6** (10 μM) cultured under normoxic conditions. Scale bars, 40 μm. Fluorescence imaging experiments were performed 1 min after the addition of the probe solution to the cells.

dx.doi.org/10.1021/ja304239g | J. Am. Chem. Soc. 2012, 134, 13386−13395

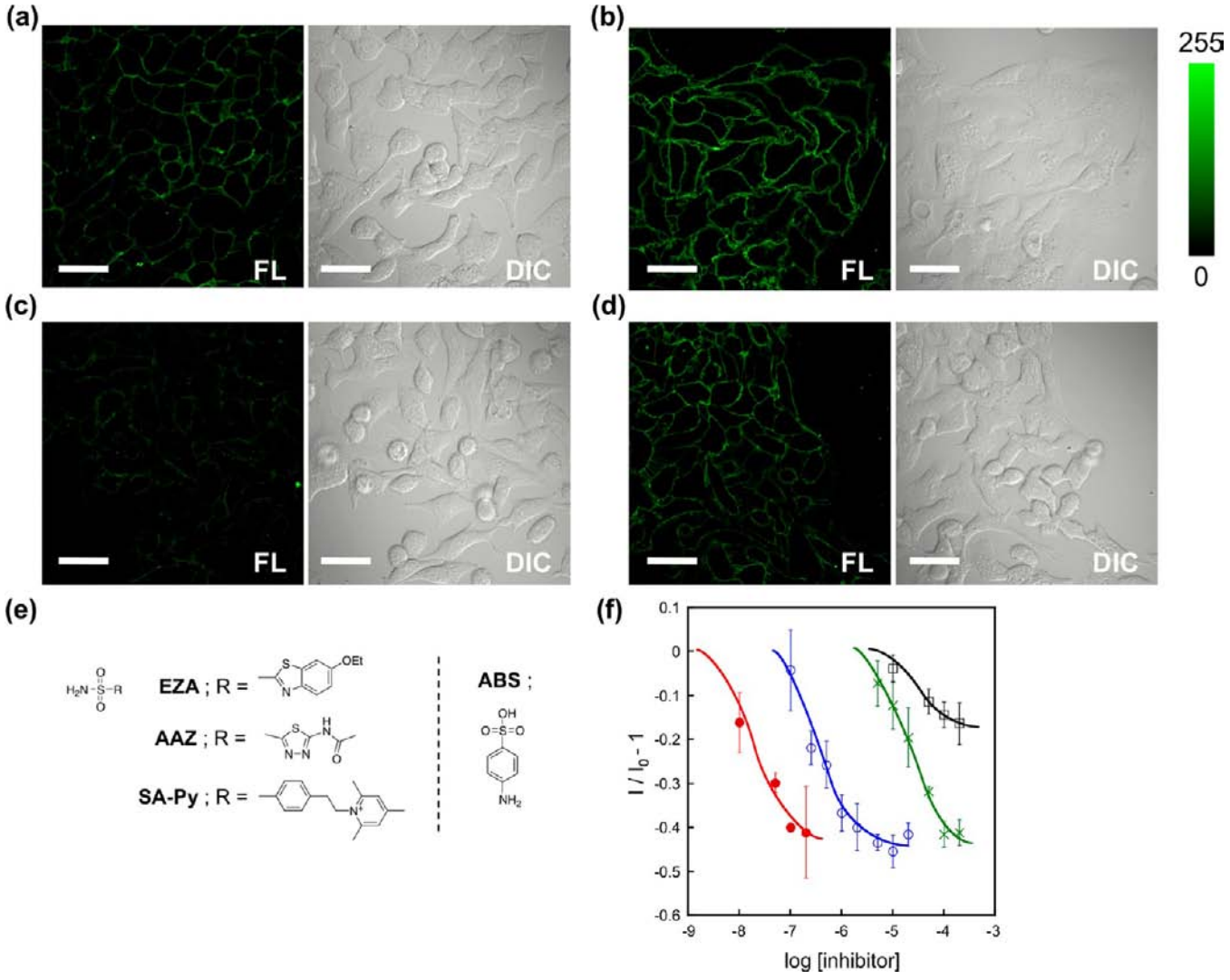

Figure 7. Imaging-based CA inhibitor cell-based assay with probe **6**. (a–d) Fluorescence images of hypoxia-cultured A549 cells treated with probe **6** (10 μM) in the presence of CA inhibitors [(a) EZA (100 nM), (b) AAZ (100 nM), (c) AAZ (5 μM), and (d) ABS (200 μM)). Scale bars, 40 μm. (e) Chemical structures of inhibitors for transmembrane-type CA used in this study. EZA is 6-ethoxy-2-benzothiazolesulfonamide, AAZ is acetazolamide, SA-Py is trimethylpyridinium derivative of benzenesulfonamide, and ABS is 4-aminobenzenesulfonic acid. (f) Fluorescence titration profile of the relative change in fluorescence intensity ($I/I_0 - 1$) from the cell surface region vs inhibitor concentration for EZA (●, red), AAZ (○, blue), SA-Py (×, green), and noninhibitor ABS (□, black). Fluorescence intensities were evaluated at five regions in each dish, and the experiments were performed in triplicate to obtain mean and standard deviation values (shown as error bars).

aminobenzenesulfonic acid (ABS), which is not a ligand for the CA family (Figure 7d). From the titration curves of these live-cell-based inhibitor assays, IC_{50} values of each inhibitor were determined to be 2.3×10^{-8} M (EZA), 2.4×10^{-7} M (AAZ), and 2.2×10^{-5} M (SA-Py) (Figure 7e and f). On the other hand, the literature values (K_i) for hCA IX were reported to be 3.4×10^{-8} M (EZA), 2.5×10^{-8} M (AAZ), and 1.4×10^{-8} M (SA-Py),[17c] the values of which were obtained by the purified system using the catalytic domain of hCA IX. While the values for EZA were almost same in the order, those for AAZ and SA-Py were apparently different. This discrepancy could be caused by the differences in these two assay systems. For example, the inhibitive capacities of AAZ and SA-Py may be decreased by the cell penetration or nonspecific binding to the cell membrane. It is conceivable that the cell-based inhibitor assays by the self-assembling probes allow us to evaluate the actual potencies in live cell settings.

CONCLUSION

In summary, we have developed self-assembling turn-on fluorescent nanoprobes that can be used for fluorescent imaging of protein biomarkers under live cell contexts, as well as in test tube settings. The design of these nanoprobes was based on recognition-driven disassembly of a ligand-tethered fluorophore, by newly introducing a hydrophobic module to finely tune the aggregation properties of the probe. This greatly enhanced the flexibility of the probe design. The probes allowed specific visualization of overexpressed FR and hypoxia-inducible CA on cancer cells, both of which are tumor-specific biomarkers, without needing any washing operations. Moreover, an extended nanoprobe was successfully used in a cell-based inhibitor assay for CA on the surface of live cells. This highlights the supramolecular approach for bioimaging under live cell conditions. Nowadays, many small-molecule drug candidates toward various membrane-bound proteins have been reported. By using such drugs, our approach using the

dx.doi.org/10.1021/ja304239g | J. Am. Chem. Soc. 2012, 134, 13386–13395

turn-on nanoprobes should be applied to the live-cell imaging of various membrane-bound proteins. We believe that the present progress in our turn-on nanoprobes should facilitate the development of various target-specific signal-switchable probes for use in cells or *in vivo*.

EXPERIMENTAL SECTION

Synthesis. Synthetic procedures used to prepare compounds **1**–**6** and **8**, and characterizations of these compounds are described in the Supporting Information. Compound **7** was prepared as previously reported.[17a]

General Materials and Methods. Purified human carbonic anhydrase II (CAII) was purchased from Sigma, and *Escherichia coli* DHFR was prepared and purified as previously reported.[19] BODIPY 558/568 SE, 5-carboxyfluorescein succinimidyl ester, and 5-carboxytetramethylrhodamine succinimidyl ester were purchased from Invitrogen/Molecular Probes. Other chemical reagents and solvents were purchased from commercial chemical suppliers (Sigma, Aldrich, TCI, Wako, or Watanabe Chemical Industries) and used without further purification. ^{1}H NMR spectra were recorded on a Varian Mercury-400 spectrometer (400 MHz). High-resolution electrospray ionization quadrupole Fourier transform mass spectrometry (HR-ESI-MS) spectra were performed on a Bruker apex-ultra (7 T) mass spectrometer. Cell imaging was performed with a confocal laser scanning microscope (CLSM, Olympus, FV1000, IX81) equipped with a 60×, NA = 1.35 oil objective lens. Fluorescence images were acquired using the 488 nm line of an argon laser to excite fluorescein (emission, 500–600 nm) and the 543 nm line of a HeNe Green laser to excite BODIPY 558/568 (emission, 550–650 nm). Measurements were carried out 1 min after staining without performing any washing operations.

UV–Visible Absorption and Fluorescence Spectroscopic Analyses. All probes were dissolved in dimethyl sulfoxide (DMSO) to generate stock solutions. The concentrations of probe **1** and **5** were determined by their absorbance (at 559 nm for **1** and 543 nm for **5**) in methanol using a molar extinction coefficient of 97,000 M^{-1} cm^{-1} for **1** and 92,000 M^{-1} cm^{-1} for **5**.[20] The concentration of fluorescein-type probes (**2**–**4** and **6**–**8**) were determined by their absorbance at 494 nm in 0.1 N NaOH aq using a molar extinction coefficient of 75,000 M^{-1} cm^{-1}.[20] hCAII was dissolved in 0.1 M Tris·HCl, and 0.1 M Na_2SO_4 buffer (pH 7.5), and DHFR was dissolved in 1 × PBS buffer (pH 7.2). The concentrations of these proteins were determined by their absorbance at 280 nm using a molar extinction coefficient of 54,000 M^{-1} cm^{-1} for hCAII,[21] and 31,100 M^{-1} cm^{-1} for DHFR,[22] allowing stock solutions of known concentrations to be prepared. All experiments were performed at 25 °C. UV–visible absorption spectra were recorded on a Shimadzu UV–visible 2550 spectrometer. Fluorescence spectra were measured using a Perkin-Elmer LS55 fluorescent spectrometer. Absorption and fluorescence measurements were performed 1 h after adding the protein to each probe solution (10 μM). The fluorescence quantum yields of probes **2**–**4** and **6**–**8** were calculated by using fluorescein (Φ = 0.85 in 0.1 N NaOH aqueous solution) as reference standard.[23]

Fluorescence Imaging with KB Cells. KB cells were maintained in folate-free RPMI 1640 medium supplemented with 10% fetal bovine serum (FBS), penicillin (100 units/mL), and streptomycin (100 μg/mL) at 37 °C in 5% CO_2 and 95% air. The cells were plated at a density of 2.0 × 10^5 cells per a 35-mm glass-bottomed dish and cultured in the medium for 24 h at 37 °C in 5% CO_2 and 95% air. The cells were rinsed with 1 × PBS buffer, and treated with probe **3** (20 μM, <1% DMSO (v/v)) or the probe **3** (20 μM) and folate (20 μM) (<1% DMSO (v/v)) in 1 × PBS buffer (1 mL). Fluorescence imaging was carried out 1 min after staining without performing any washing operations. For the control experiment, a DHFR stock solution was added to cells stained with the probe **3** only to give a final concentration of 5 μM, and then fluorescence imaging was carried out without removing the probe.

Fluorescence Imaging with A549 Cells. A549 cells were maintained in DMEM supplemented with 10% FBS, penicillin (100 units/mL), and streptomycin (100 μg/mL) at 37 °C in 5% CO_2 and 95% air. The cells were plated at a density of 2.0 × 10^5 cells per a 35-mm glass-bottomed dish and cultured for 24 h at 37 °C in air with 5% CO_2. After the medium exchange, the cells were cultured for 24 h at 37 °C under hypoxic conditions (<0.1% O_2) generated with an AnaeroPack (Mitsubishi Gas Chemical Company. Inc.) and a rectangular jar. For control experiments, parallel normoxic dishes were incubated in DMEM with or without DFO (200 μM) for 24 h at 37 °C in air with 5% CO_2. The cells were rinsed with 1 × PBS buffer, and then treated with the probe **6** (10 μM, <1% DMSO (v/v)] or the probe **6** (10 μM) and EZA (100 μM) (<1% DMSO (v/v)] in 1 × PBS buffer (1 mL). Fluorescence imaging was carried out 1 min after staining without performing any washing operations.

Inhibitor Assay for Membrane-Bound hCA Family on A549 Cells. The concentration of probe **6** was fixed at 10 μM in each experiment. After adding probe **6** to the A549 cells cultured under hypoxic conditions as described above, a stock solution of each inhibitor was added to the cells stained with the probe and fluorescence imaging was carried out without performing any washing operations. To determine the fluorescence intensity on the cell membrane, CLSM images were analyzed with ImageJ 1.44 on a Macintosh PC.

ASSOCIATED CONTENT

Supporting Information

Figures S1–S8, experimental details, and synthesis procedures. This material is available free of charge via the Internet at http://pubs.acs.org.

AUTHOR INFORMATION

Corresponding Author

ihamachi@sbchem.kyoto-u.ac.jp

Notes

The authors declare no competing financial interest.

ACKNOWLEDGMENTS

Prof. Teruyuki Nagamune (The University of Tokyo) and Dr. Shinya Tsukiji (Nagaoka University of Technology) are thanked for the plasmid encoding pBAD-DHFR. Prof. K. Matsuda (Kyoto University) and Dr. M. Ikeda (Kyoto University, Hamachi Lab) are acknowledged for their help with DLS and AFM measurements, respectively. K.M. acknowledges JSPS Research Fellowships for Young Scientists. This work was partly supported by the CK Integrated Medical Bioimaging Project (MEXT) and CREST (Japan Science and Technology Agency).

REFERENCES

(1) Grimm, D.; Bauer, J.; Pietsch, J.; Infanger, M.; Eucker, J.; Eilles, C.; Schoenberger, J. *Curr. Med. Chem.* **2011**, *18*, 176–190.

(2) Kobayashi, H.; Ogawa, M.; Alford, R.; Choyke, P. L.; Urano, Y. *Chem. Rev.* **2010**, *110*, 2620–2640.

(3) Urano, Y.; Asanuma, D.; Hama, Y.; Koyama, Y.; Barrett, T.; Kamiya, M.; Nagano, T.; Watanabe, T.; Hasegawa, A.; Choyke, P. L.; Kobayashi, H. *Nat. Med.* **2009**, *15*, 104–109.

(4) (a) Gao, W.; Xing, B.; Tsien, R. Y.; Rao, J. *J. Am. Chem. Soc.* **2003**, *125*, 11146–11147. (b) Kamiya, M.; Kobayashi, H.; Hama, Y.; Koyama, Y.; Bernardo, M.; Nagano, T.; Choyke, P. L.; Urano, Y. *J. Am. Chem. Soc.* **2007**, *129*, 3918–3929.

(5) (a) Zlokarnik, G.; Negulescu, P. A.; Knapp, T. E.; Mere, L.; Burres, N.; Feng, L.; Whitney, M.; Roemer, K.; Tsien, R. Y. *Science* **1998**, *279*, 84–88. (b) Mizukami, S.; Kikuchi, K.; Higuchi, T.; Urano, Y.; Mashima, T.; Tsuruo, T.; Nagano, T. *FEBS Lett.* **1999**, *453*, 356–360. (c) Takakusa, H.; Kikuchi, K.; Urano, Y.; Sakamoto, S.; Yamaguchi, K.; Nagano, T. *J. Am. Chem. Soc.* **2002**, *124*, 1653–1657. (d) Pham, W.; Choi, Y.; Weissleder, R.; Tung, C. -H.

Bioconjugate Chem. **2004**, *15*, 1403−1407. (e) Lawrence, D. S.; Wang, Q. *ChemBioChem* **2007**, *8*, 373−378.
(6) (a) You, C.-C.; Miranda, O. R.; Gider, B.; Ghosh, P. S.; Kim, I.-B.; Erdogan, B.; Krovi, S. A.; Bunz, U. H. F.; Rotello, V. M. *Nat. Nanotechnol.* **2007**, *2*, 318−323. (b) De, M.; Rana, S.; Akpinar, H.; Miranda, O. R.; Arvizo, R. R.; Bunz, U. H. F.; Rotello, V. M. *Nature Chem.* **2009**, *1*, 461−465. (c) Bajaj, A.; Miranda, O. R.; Kim, I.-B.; Phillips, R. L.; Jerry, D. J.; Bunz, U. H. F.; Rotello, V. M. *Proc. Natl. Acad. Sci. U.S.A.* **2009**, *106*, 10912−10916. (d) Miranda, O. R.; Chen, H.-T.; You, C.-C.; Mortenson, D. E.; Yang, X.-C.; Bunz, U. H. F.; Rotello, V. M. *J. Am. Chem. Soc.* **2010**, *132*, 5285−5289.
(7) (a) Savariar, E. N.; Ghosh, S.; González, D. C.; Thayumanavan, S. *J. Am. Chem. Soc.* **2008**, *130*, 5416−5417. (b) Azagarsamy, M. A.; Sokkalingam, P.; Thayumanavan, S. *J. Am. Chem. Soc.* **2009**, *131*, 14184−14185. (c) Azagarsamy, M. A.; Yesilyurt, V.; Thayumanavan, S. *J. Am. Chem. Soc.* **2010**, *132*, 4550−4551. (d) Yesilyurt, V.; Ramireddy, R.; Azagarsamy, M. A.; Thayumanavan, S. *Chem.—Eur. J.* **2012**, *18*, 223−229. (e) Das, G.; Talukdar, P.; Matile, S. *Science* **2002**, *298*, 1600−1602. (f) Sorde, N.; Das, G.; Matile, S. *Proc. Natl. Acad. Sci. U.S.A.* **2003**, *100*, 11964−11969.
(8) (a) Takaoka, Y.; Sakamoto, T.; Tsukiji, S.; Narazaki, M.; Matsuda, T.; Tochio, H.; Shirakawa, M.; Hamachi, I. *Nature Chem.* **2009**, *1*, 557−561. (b) Takaoka, Y.; Kiminami, K.; Mizusawa, K.; Matsuo, K.; Narazaki, M.; Matsuda, T.; Hamachi, I. *J. Am. Chem. Soc.* **2011**, *133*, 11725−11731.
(9) Mizusawa, K.; Ishida, Y.; Takaoka, Y.; Miyagawa, M.; Tsukiji, S.; Hamachi, I. *J. Am. Chem. Soc.* **2010**, *132*, 7291−7293.
(10) (a) Antony, A. C. *Annu. Rev. Nutr.* **1996**, *16*, 501−521. (b) Sudimack, J.; Lee, R. J. *Adv. Drug. Delivery Rev.* **2000**, *41*, 147−162. (c) Xia, W.; Low, P. S. *J. Med. Chem.* **2010**, *53*, 6811−6824.
(11) Rijinboutt, S.; Jansen, G.; Posthuma, G.; Hynes, J. B.; Schornagel, J. H.; Strous, G. J. *J. Cell. Biol.* **1996**, *132*, 35−47.
(12) (a) Matthews, D. A.; Alden, R. A.; Bolin, J. T.; Freer, S. T.; Hamlin, R.; Xuong, N.; Kraut, J.; Poe, M.; Williams, M.; Hoogsteen, K. *Science* **1977**, *197*, 452−455. (b) Miller, L. W.; Sable, J.; Goelet, P.; Sheetz, M. P.; Cornish, V. W. *Angew. Chem., Int. Ed.* **2004**, *43*, 1672−1675.
(13) (a) Turek, J. J.; Leamon, C. P.; Low, P. S. *J. Cell. Sci.* **1993**, *106*, 423−430. (b) Quintana, A.; Raczka, E.; Piehler, L.; Lee, I.; Myc, A.; Majoros, I.; Patri, A. K.; Thomas, T.; Mulé, J.; Baker, J. R., Jr. *Pharm. Res.* **2002**, *19*, 1310−1316. (c) Kukowska-Latallo, J. F.; Candido, K. A.; Cao, Z.; Nigavekar, S. S.; Majoros, I. J.; Thomas, T. P.; Balogh, L. P.; Khan, M. K.; Baker, J. R., Jr. *Cancer Res.* **2005**, *65*, 5317−5324.
(14) Rosenholm, J. M.; Meinander, A.; Peuhu, E.; Niemi, R.; Eriksson, J. E.; Sahlgren, C.; Lindén, M. *ACS Nano* **2009**, *3*, 197−206.
(15) (a) Wykoff, C. C.; Beasley, N. J. P.; Watson, P. H.; Turner, K. J.; Pastorek, J.; Sibtain, A.; Wilson, G. D.; Turley, H.; Talks, K. L.; Maxwell, P. H.; Pugh, C. W.; Ratcliffe, P. J.; Harris, A. L. *Cancer Res.* **2000**, *60*, 7075−7083. (b) Ivanov, S.; Liao, S.-Y.; Ivanova, A.; Danilkovitch-Miagkova, A.; Tarasova, N.; Weirich, G.; Merrill, M. J.; Proescholdt, M. A.; Oldfield, E. H.; Lee, J.; Zavada, J.; Waheed, A.; Sly, W.; Lerman, M. I.; Stanbridge, E. J. *Am. J. Pathol.* **2001**, *158*, 905−919.
(16) (a) Svastova, E.; Zilka, N.; Zat'ovicova, M.; Gibadulinova, A.; Ciampor, F.; Pastorek, J.; Pastorekova, S. *Exp. Cell. Res.* **2003**, *290*, 332−345. (b) Svastova, E.; Hulikova, A.; Rafajova, M.; Zat'ovicova, M.; Gibadulinova, A.; Casini, A.; Cecchi, A.; Scozzafava, A.; Supuran, C. T.; Pastorek, J.; Pastorekova, S. *FEBS lett.* **2004**, *577*, 439−445. (c) Robertson, N.; Potter, C.; Harris, A. L. *Cancer Res.* **2004**, *64*, 6160−6165. (d) Chiche, J.; Ilc, K.; Laferriere, J.; Trottier, E.; Dayan, F.; Mazure, N. M.; Brahimi-Horn, M. C.; Pouyssegur, J. *Cancer Res.* **2009**, *69*, 358−368.
(17) (a) Cecchi, A.; Hulikova, A.; Pastorek, J.; Pastorekova, S.; Scozzafava, A.; Winum, J. Y.; Montero, J. L.; Supuran, C. T. *J. Med. Chem.* **2005**, *48*, 4834−4841. (b) Thiry, A.; Dogné, J. -M.; Masereel, B.; Supuran, C. T. *Trends Pharmacol. Sci.* **2006**, *27*, 566−573. (c) Supuran, C. T. *Nat. Rev. Drug. Discov.* **2008**, *7*, 168−181. (d) Simone, G. D.; Supuran, C. T. *Biochim. Biophys. Acta* **2010**, *1804*, 404−409.
(18) In CA imaging, a half of the concentration of the probe was used relative to FR imaging. Thus the background fluorescence derived from the probe aggregates was lower in the extracellular region in Figure 6a than Figure 5a.
(19) Tanaka, T.; Kamiya, N.; Nagamune, T. *FEBS Lett.* **2005**, *579*, 2092−2096.
(20) Haugland, R. P. *The Handbook: A Guide to Fluorescent Probes and Labeling Technologies*, 10th ed.; Invitrogen: Carlsbad, CA, 2005.
(21) Supuran, C. T.; Briganti, F.; Tilli, S.; Chegwidden, W. R.; Scozzafava, A. *Bioorg. Med. Chem.* **2001**, *9*, 703−714.
(22) Touchette, N. A.; Perry, K. M.; Matthews, C. R. *Biochemistry* **1986**, *25*, 5445−5452.
(23) Parker, C. A.; Rees, W. T. *Analyst* **1960**, *85*, 587−600.